hydroxyprolyl residues. The details of these will be published elsewhere.

Acknowledgment. This work was partly supported by a research grant from Department of Science and Technology, Government of India, and PL-480-USPHS Grant No. 01-126-N.

References and Notes

(1) L. Pauling, R. B. Corey, and H. R. Branson, *Proc. Natl. Acad. Sci. U.S.A.*, **37**, 205 (1951).
(2) L. Pauling and R. B. Corey, *Proc. Natl. Acad. Sci. U.S.A.*, **39**, 253 (1953).
(3) G. N. Ramachandran and G. Kartha, *Nature (London)*, **176**, 593 (1955).
(4) G. N. Ramachandran and V. Sasisekharan, *Adv. Protein Chem.*, **23**, 283 (1968).
(5) F. H. C. Crick and A. Rich, *Nature (London)*, **176**, 780 (1955).
(6) V. Sasisekharan, *Acta Crystallogr.*, **12**, 897 (1959).
(7) E. Bendetti in "Proceedings of the Fifth American Peptide Symposium", M. Goodman and J. Meienhofer, Eds., Wiley, New York, N.Y., 1977, p 257.
(8) E. M. Bradbury, L. Brown, A. R. Downie, A. Elliott, R. D. B. Fraser, and W. E. Hanby, *J. Mol. Biol.*, **5**, 230 (1962).
(9) C. Ramakrishnan and N. Prasad, *Int. J. Protein Res.*, **3**, 209 (1971).
(10) C. H. Bamford, L. Brown, A. Elliott, W. E. Hanby, and I. F. Trotter, *Nature (London)*, **171**, 1149 (1953).
(11) C. H. Bamford, L. Brown, E. M. Cant, A. Elliott, W. E. Hanby, and B. R. Malcolm, *Nature (London)*, **176**, 396 (1955).
(12) B. Lotz, *J. Mol. Biol.*, **87**, 169 (1974).
(13) F. J. Padden and H. D. Keith, *J. Appl. Phys.*, **36**, 2987 (1965).
(14) T. Miyazawa in "Poly-α-Amino Acids", G. D. Fasman, Ed., Marcel Dekker, New York, N.Y., 1967, Chapter 2.
(15) F. Colonna-Cesari, S. Premilat, and B. Lotz, *J. Mol. Biol.*, **87**, 181 (1974).
(16) G. N. Ramachandran, C. Ramakrishnan, and C. M. Venkatachalam in "Conformation of Biopolymers", Vol. 2, G. N. Ramachandran, Ed., Academic Press, New York, N.Y., 1967, p 429.
(17) R. A. Scott and H. A. Scheraga, *J. Chem. Phys.*, **45**, 2091 (1966).
(18) C. M. Venkatachalam, B. J. Price, and S. Krimm, *Macromolecules*, **7**, 212 (1974).
(19) P. M. Cowan and S. McGavin, *Nature (London)*, **176**, 501 (1955).
(20) V. Sasisekharan, *J. Polym. Sci.*, **47**, 373 (1960).
(21) W. Traub and U. Shmueli in "Aspects of Protein Structure", G. N. Ramachandran, Ed., Academic Press, New York, N.Y., 1963, p 81.
(22) W. Traub and U. Shmueli, *Nature (London)*, **198**, 1165 (1963).
(23) I. Z. Steinberg, W. F. Harrington, A. Berger, M. Sela, and E. Katchalaski, *J. Am. Chem. Soc.*, **82**, 5263 (1960).
(24) P. De Santis, E. Giglio, A. M. Liquori, and A. Ripamonti, *Nature (London)*, **201**, 456 (1965).
(25) P. R. Schimmel and P. J. Flory, *Proc. Natl. Acad. Sci. U.S.A.*, **58**, 52 (1967).
(26) N. Gō and H. A. Scheraga, *Macromolecules*, **3**, 188 (1970).
(27) W. L. Mattice, K. Nishikawa, and T. Ooi, *Macromolecules*, **6**, 443 (1973).
(28) G. Schilling and Kricheldorf, *Makromol. Chem.*, **178**, 885 (1977).
(29) W. L. Mattice and L. Mandelkern, *Biochemistry*, **10**, 1926 (1971).
(30) D. A. Torchia, *Biochemistry*, **11**, 1462 (1972).
(31) D. A. Torchia and J. R. Lyerla, Jr., *Biopolymers*, **13**, 97 (1974).
(32) D. A. Rabenold, W. L. Mattice, and L. Mandelkern, *Macromolecules*, **7**, 43 (1974).

Transport Coefficients of Helical Wormlike Chains. 2. Translational Friction Coefficient

Hiromi Yamakawa* and Takenao Yoshizaki

Department of Polymer Chemistry, Kyoto University, Kyoto, Japan.
Received October 4, 1978

ABSTRACT: The translational friction coefficient of the helical wormlike chain is evaluated by an application of the Oseen–Burgers procedure of hydrodynamics to the cylinder model. The Oseen hydrodynamic interaction tensor is preaveraged, and therefore there is no need of consideration of the effect of the coupling between translational and rotational motions. A useful empirical interpolation formula is also derived to be valid for any possible values of the model parameters. Some salient aspects of the behavior of the sedimentation coefficient are discussed on the basis of the numerical results. In particular, it is pointed out that even if the proportionality of the sedimentation coefficient to the square root of the molecular weight is experimentally observed over a wide range, the chain may not always be regarded as a random coil but may possibly be characterized as a helical wormlike chain.

In a previous paper,[1] part 1 of this series, a study of the steady-state transport coefficients of helical wormlike (HW) chains[2,3] (without excluded volume) was initiated. The evaluation of the translational diffusion (or friction) coefficient and intrinsic viscosity of the characteristic regular helix,[3] i.e., one of the three extreme forms of the model chain corresponding to its minimum configurational energy, was carried out by an application of the Oseen–Burgers procedure of hydrodynamics[4] to cylinder models. In this paper, we proceed to evaluate the translational friction coefficient of HW chains along the same line.

As discussed in detail previously,[1] there are two fundamental problems to be considered. One is concerned with the steady-state transport length scales for the cylinder model, and the other with the possible effect of the coupling between translational and rotational motions of skew bodies. The length scales to be adopted must be of the same order as or larger than those associated with the equilibrium chain configurations. This should always be kept in mind when an analysis of experimental data is made by the use of theoretical expressions for the transport coefficients derived in the present and later papers. As for the second problem, it was shown that if the Oseen hydrodynamic interaction tensor is preaveraged in the Kirkwood–Riseman scheme,[5] the coupling does not affect the translational friction coefficient of the regular helix at all, while the effect on its intrinsic viscosity may be negligibly small except when the number of its turns is very small. It is clear that the skewness is partly destroyed for the HW chain having internal degrees of freedom, and moreover, the evaluation for this chain is carried out with the preaveraged Oseen tensor as in the case of the Kratky–Porod (KP) wormlike chain.[4] Therefore, we do not consider the coupling in the present and later papers.

The mean reciprocal distance between two contour points of the chain, which is necessary for the evaluation

0024-9297/79/2212-0032$01.00/0

with the preaveraged Oseen tensor, has already been obtained in closed form for several cases of the values of the model parameters.[6] Thus, in section I, we derive a semianalytical expression for the translational friction coefficient by the well-established method. In section II, we consider the associated KP chain,[3] i.e., the KP chain whose Kuhn length is the same as that of the HW chain under consideration. This serves to derive in section III an empirical interpolation formula for the translational friction coefficient of the latter which is valid for any possible values of the model parameters. In section IV, we discuss some salient aspects of the behavior of the sedimentation coefficient on the basis of the numerical results. An analysis of experimental data is deferred to the next paper, in which the intrinsic viscosity is studied.

Basic Equations

Until the molecular weight is explicitly introduced, the equilibrium average configuration of the HW chain of a given contour length may be described by four parameters: the constant curvature κ_0 and torsion τ_0 of the characteristic helix, the Kuhn length λ^{-1} of the KP chain as defined as the HW chain with $\kappa_0 = 0$, and Poisson's ratio σ. Most of the numerical computations were carried out for $\sigma = 0$, and therefore we consider this particular case also in this paper. (Note that the moments of the end-to-end distance are rather insensitive to the change in σ.) The HW cylinder as the hydrodynamic model is defined by further introducing the total length L and the diameter d of the cylinder. It reduces to the regular helical cylinder studied in part 1, in the limit $\lambda \to 0$, λ^{-1} being a measure of chain stiffness. In what follows, all lengths are measured in units of λ^{-1} unless specified otherwise. It is sometimes convenient to use instead of κ_0 and τ_0 the parameters μ and ν defined by

$$\mu = \tau_0(\kappa_0^2 + \tau_0^2)^{-1/2}$$
$$\nu = (\kappa_0^2 + \tau_0^2)^{1/2} \tag{1}$$

as in part 1. The parameter μ determines the form of the characteristic regular helix apart from its size, i.e., the ratio h/ρ of its pitch h to radius ρ (whether the reduced or unreduced lengths are used), and $\nu/2\pi$ is equal to the number of its turns contained in the unreduced contour length equal to λ^{-1} (in the unit contour length when the unreduced lengths are used). Note that the (reduced) parameters κ_0, τ_0, and ν increase to infinity as λ is decreased to zero.

Now, we suppose that the HW cylinder possesses the uniform translational velocity $\mathbf{U}$ in a solvent with viscosity coefficient η_0, whose unperturbed flow field is nonexistent, and we replace the cylinder by a frictional force distribution $\mathbf{f}(x)$ per unit length along the cylinder axis as a function of the contour distance x ($0 \le x \le L$) from one end, following the Oseen–Burgers procedure. If the Oseen tensor is preaveraged, there is no need of consideration of the coupling effect arising from the chain skewness, so that the configurational average $\langle \mathbf{f}(x) \rangle$ of the frictional force satisfies formally the same integral equation as in the case of the KP cylinder,[4]

$$\int_0^L K(x,y)\langle \mathbf{f}(y) \rangle \, dy = 6\pi\eta_0\mathbf{U} \tag{2}$$

with

$$K(x,y) = K(|x - y|) = \langle |\mathbf{R} - \mathbf{r}|^{-1} \rangle \tag{3}$$

where $\mathbf{R}$ is the distance between the contour points x and y, $\mathbf{r}$ is the normal radius vector from the contour point x to the cylinder surface, so that $|\mathbf{r}| = d/2$, and in eq 3 the $\langle\rangle$ denotes the configurational average and also the average over $\mathbf{r}$. The mean total frictional force $\langle \mathbf{F} \rangle$ and the translational friction coefficient Ξ are given by

$$\langle \mathbf{F} \rangle = \Xi\mathbf{U} = \int_0^L \langle \mathbf{f}(x) \rangle \, dx \tag{4}$$

If the solution of eq 2 in the Kirkwood–Riseman approximation is substituted into eq 4, we obtain for Ξ

$$3\pi\eta_0 L/\Xi = L^{-1}\int_0^L (L - t)K(t) \, dt \tag{5}$$

with $t = |x - y|$. Thus, the problem is to evaluate the kernel $K(t) = \langle |\mathbf{R} - \mathbf{r}|^{-1} \rangle$ and the integral in eq 5.

Statistical mechanically, the HW chain of contour length t may be described completely by the Green's function $G(\mathbf{R},\mathbf{u},\mathbf{a}|\mathbf{u}_0,\mathbf{a}_0;t)$, i.e., the conditional distribution function of the radius vector $\mathbf{R}(t) = \mathbf{R}$ of the contour, the unit tangent vector $\mathbf{u}(t) = \mathbf{u}$, and the unit mean curvature vector $\mathbf{a}(t) = \mathbf{a}$ when $\mathbf{R}(0) = 0$, $\mathbf{u}(0) = \mathbf{u}_0$, and $\mathbf{a}(0) = \mathbf{a}_0$.[2,7,8] The kernel, or the mean reciprocal distance, may then be evaluated from

$$K(t) = (2\pi)^{-1}\int d\mathbf{R} \int' d\mathbf{r}|\mathbf{R} - \mathbf{r}|^{-1}G(\mathbf{R}|\mathbf{u}_0,\mathbf{a}_0;t) \tag{6}$$

with

$$G(\mathbf{R}|\mathbf{u}_0,\mathbf{a}_0;t) = \int G(\mathbf{R},\mathbf{u},\mathbf{a}|\mathbf{u}_0,\mathbf{a}_0;t) \, d\mathbf{u} \, d\mathbf{a} \tag{7}$$

where the integral over $\mathbf{r}$ is subject to the condition,

$$\mathbf{r}\cdot\mathbf{u}_0 = 0 \tag{8}$$

The set of unit vectors $\mathbf{a}$, $\mathbf{b}$ ($=\mathbf{u} \times \mathbf{a}$), and $\mathbf{u}$ defines a localized Cartesian coordinate system affixed to the chain, whose axes coincide with the local principal axes of inertia of the chain as an elastic wire.[8] It is then clear that $K(t)$ is independent of the orientation of the initial localized system $(\mathbf{a}_0,\mathbf{b}_0,\mathbf{u}_0)$, and also that the directions of $\mathbf{r}$ and $\mathbf{a}_0$, which are perpendicular to $\mathbf{u}_0$, are independent of each other, $\mathbf{r}$ being just the normal radius vector introduced in the application of the Oseen–Burgers procedure to the hydrodynamic cylinder model. We therefore have

$$K(t) = (2\pi)^{-1}\int d\mathbf{R} \int' d\mathbf{r}|\mathbf{R} - \mathbf{r}|^{-1}G(\mathbf{R}|\mathbf{u}_0=\mathbf{e}_z;t) \tag{9}$$

where $\mathbf{e}_z$ is the unit vector in the direction of the z axis of an external Cartesian coordinate system, and

$$G(\mathbf{R}|\mathbf{u}_0;t) = (2\pi)^{-1}\int G(\mathbf{R}|\mathbf{u}_0,\mathbf{a}_0;t) \, d\mathbf{a}_0 \tag{10}$$

An approximate expression for the mean reciprocal distance given by eq 9 has already been found to be (eq 66 of ref 6)

$$K(t) = (t^2 + \tfrac{1}{4}d^2)^{-1/2}\left(1 + \sum_{i=1}^{5} f_{i0}t^i + \sum_{i=1}^{3}\sum_{j=1}^{2} f_{ij}d^{2j}t^i\right) \qquad \text{for } t \le \sigma_1$$

$$K(t) = (6/\pi c_\infty t)^{1/2}\sum_{i=0}^{2}\sum_{j=0}^{i} B_{ij}\, d^{2j}(c_\infty t)^{-i} + h(\sigma_2 - t)(c_\infty t)^{-1/2}\sum_{i=0}^{q}\sum_{j=0}^{2} E_{ij}d^{2j}(t - \sigma_2)^{i+3} \qquad \text{for } t > \sigma_1 \tag{11}$$

with

$$f_{10} = 1/3, \qquad B_{00} = 1, \qquad B_{11} = -0.125, \qquad B_{22} = 0.0140625 \tag{12}$$

where $h(x)$ is the unit step function defined by $h(x) = 1$ for $x \ge 0$ and $h(x) = 0$ for $x < 0$; and σ_1, σ_2, f_{i0} (i = 2–5), f_{ij} (i = 1–3; j = 1, 2), B_{10}, B_{20}, B_{21}, E_{ij}, and q are constants

independent of t and d but dependent on κ_0 and τ_0 and to be determined numerically to give a good approximation to $K(t)$ (for the details, see ref 6). c_∞ is the Kuhn length of the HW chain (for $\sigma = 0$) and is given by[2,3]

$$c_\infty = \lim_{t\to\infty}(\langle R^2\rangle/t) = \frac{4+\tau_0^2}{4+\kappa_0^2+\tau_0^2} = \frac{4+\mu^2\nu^2}{4+\nu^2} \qquad (\sigma = 0) \quad (13)$$

with $\langle R^2\rangle$ the mean-square end-to-end distance of the chain of contour length t. Note that $\sigma_1 = \sigma_2$ and $f_{40} = f_{50} = E_{ij} = 0$ for the KP chain with $\kappa_0 = 0$.

Substitution of eq 11 into eq 5 and integration leads to

$$3\pi\eta_0 L/\Xi = F_1(L,d;L_1) + h(L-\sigma_1)F_2(L,d;L_2,\sigma_1,\sigma_2) + h(L-\sigma_1)F_3(L,d;\sigma_1) \quad (14)$$

where F_i are defined by

$$F_1(L,d;L_1) = \sum_{i=0}^{5} f_{i0}L_1^i[I_i(d/L_1) - (L_1/L)I_{i+1}(d/L_1)] + \sum_{i=1}^{3}\sum_{j=1}^{2} f_{ij}L_1^i d^{2j}[I_i(d/L_1) - (L_1/L)I_{i+1}(d/L_1)] \quad (15)$$

$$F_2(L,d;L_2,\sigma_1,\sigma_2) = c_\infty^{-1/2}\sum_{i=0}^{q}\sum_{j=0}^{2} E_{ij}d^{2j}\sum_{r=0}^{i+3}\binom{i+3}{r}(-\sigma_2)^r \times \left\{\left[\frac{1}{i-r+7/2} - \frac{L_2}{L(i-r+9/2)}\right]L_2^{\,i-r+7/2} - \left[\frac{1}{i-r+7/2} - \frac{\sigma_1}{L(i-r+9/2)}\right]\sigma_1^{\,i-r+7/2}\right\} \quad (16)$$

$$F_3(L,d;\sigma_1) = \left(\frac{6}{\pi c_\infty}\right)^{1/2}\sum_{i=0}^{2}\sum_{j=0}^{i} B_{ij}d^{2j}c_\infty^{-i}\left\{\frac{L^{1/2-i}}{(i-1/2)(i-3/2)} + \left[\frac{1}{i-1/2} - \frac{\sigma_1}{L(i-3/2)}\right]\sigma_1^{\,1/2-i}\right\} \quad (17)$$

with

$$f_{00} = 1 \quad (18)$$

$$L_i = L \text{ for } L \le \sigma_i \ (i = 1,2); \quad L_i = \sigma_i \text{ for } L > \sigma_i \ (i = 1,2) \quad (19)$$

$$I_0(x) = -\ln x + \ln 2 + \ln[1 + (1 + \tfrac{1}{4}x^2)^{1/2}]$$
$$I_1(x) = (1 + \tfrac{1}{4}x^2)^{1/2} - \tfrac{1}{2}x$$
$$I_2(x) = \tfrac{1}{2}(1 + \tfrac{1}{4}x^2)^{1/2} - \tfrac{1}{8}x^2 I_0(x)$$
$$I_3(x) = \tfrac{1}{3}(1 + \tfrac{1}{4}x^2)^{1/2} - \tfrac{1}{6}x^2 I_1(x)$$
$$I_4(x) = \tfrac{1}{4}(1 - \tfrac{3}{8}x^2)(1 + \tfrac{1}{4}x^2)^{1/2} + \tfrac{3}{128}x^4 I_0(x)$$
$$I_5(x) = \tfrac{1}{5}(1 - \tfrac{1}{3}x^2)(1 + \tfrac{1}{4}x^2)^{1/2} + \tfrac{1}{30}x^4 I_1(x)$$
$$I_6(x) = \tfrac{1}{6}(1 - \tfrac{5}{16}x^2 + \tfrac{15}{128}x^4)(1 + \tfrac{1}{4}x^2)^{1/2} - \tfrac{5}{1024}x^6 I_0(x) \quad (20)$$

Equation 14 for Ξ is semianalytical since the involved constants f_{ij}, E_{ij}, B_{ij}, etc., have been evaluated only for several cases of the values of κ_0 and τ_0, and moreover, it is not convenient for practical use because of its complexity. Therefore, we reconstruct a simpler and completely analytical interpolation formula for Ξ approximately on the basis of its values calculated from eq 14. For this purpose, the constants above must be evaluated systematically for more cases of the values of κ_0 and τ_0. Before proceeding to do this, in the next section we examine the behavior of Ξ for the associated KP chain whose Kuhn length is equal to c_∞ and which corresponds to the base of the triangle in our hypothesis on polymer chain configurations (see Figure 1 of ref 3).

In what follows, it is convenient to designate the left-hand side of eq 5 or 14 by $\bar{s}$,

$$\bar{s} = 3\pi\eta_0 L/\Xi \quad (21)$$

which is related to the experimentally observable (unreduced) translational diffusion coefficient D and sedimentation coefficient s by

$$D = \lambda kT\bar{s}/3\pi\eta_0 L \quad (22)$$

$$s = \lambda M(1 - \bar{v}\rho_0)\bar{s}/3\pi\eta_0 L N_A \quad (23)$$

where k is the Boltzmann constant, T the absolute temperature, N_A the Avogadro number, M the molecular weight of the solute, $\bar{v}$ its partial specific volume, and ρ_0 the mass density of the solvent. Note that $\bar{s}$ is proportional to s.

The Associated KP Chain

An expression for any average quantity for the associated KP chain may be obtained from the corresponding expression for the KP chain by further reducing all (reduced) lengths l by c_∞, i.e., by replacing l by $c_\infty^{-1}l$. Therefore, the kernel $K_{a\text{-}KP}(t,d)$, or the mean reciprocal distance, as a function of t and d for the associated KP chain may be obtained from the kernel $K_{KP}(t,d)$ for the KP chain as

$$K_{a\text{-}KP}(t,d) = c_\infty^{-1}K_{KP}(c_\infty^{-1}t, c_\infty^{-1}d) \quad (24)$$

By the use of eq 37 of ref 4 for $K_{KP}(t,d)$ in eq 24, we then find, from eq 5, for $\bar{s}_{a\text{-}KP}$, i.e., the quantity $\bar{s}$ defined by eq 21 with $\Xi_{a\text{-}KP}$ for the associated KP chain

$$\bar{s}_{a\text{-}KP}(L,d;\sigma_1) = F_1(L,d;L_1) + h(L-\sigma_1)F_3(L,d;\sigma_1) \quad (25)$$

where F_1 and F_3 are defined by eq 15 and 17 with B_{00}, B_{11}, B_{22}, f_{00}, and L_1 being given by eq 12, 18, and 19 but with σ_1 and the remaining coefficients by

$$\sigma_1 = 2.278c_\infty, \quad f_{10} = \tfrac{1}{3}c_\infty^{-1}, \quad f_{20} = 0.1130c_\infty^{-2}, \quad f_{30} = -0.02447c_\infty^{-3}, \quad f_{40} = f_{50} = 0,$$
$$f_{11} = 0.04080c_\infty^{-3}, \quad f_{12} = 0.004898c_\infty^{-5}, \quad f_{21} = -0.4736c_\infty^{-4}, \quad f_{22} = -0.002270c_\infty^{-6},$$
$$f_{31} = 0.009666c_\infty^{-5}, \quad f_{32} = 0.0002060c_\infty^{-7}, \quad B_{10} = -0.025c_\infty^{2}, \quad B_{20} = -0.016295c_\infty^{4},$$
$$B_{21} = 0.065625c_\infty^{2} \quad (26)$$

Note that σ in eq 37 of ref 4 for the KP chain is equal to $\sigma_1 = 2.278$ (with $c_\infty = 1$), and therefore that in the use of this equation in eq 24, the inequalities $t > \sigma$ or $t < \sigma$ for the KP chain should be replaced by $t > \sigma_1$ or $t < \sigma_1$ with $\sigma_1 = 2.278c_\infty$.

As seen from eq 5 and 24, the $\bar{s}_{a\text{-}KP}$ given by eq 25 is equal to the quantity $\bar{s}_{KP}(L,d;\sigma_1)$ for the KP chain with $c_\infty^{-1}L$ and $c_\infty^{-1}d$ in place of L and d, respectively,

$$\bar{s}_{a\text{-}KP}(L,d;\sigma_1) = \bar{s}_{KP}(c_\infty^{-1}L, c_\infty^{-1}d;\sigma_1) \quad (27)$$

where $\sigma_1 = 2.278$ on the right-hand side of eq 27, so that $\bar{s}_{a\text{-}KP}$ reduces to $\bar{s}_{KP}$ when $\kappa_0 = 0$, and therefore when $c_\infty = 1$. Note that the previous results for the KP chain given in ref 4 may be obtained by expanding the $\bar{s}_{a\text{-}KP}$ given by eq 25 with $c_\infty = 1$ in powers of d/L and d, assuming that $d/L \ll 1$ and $d \ll 1$. However, we avoid this expansion

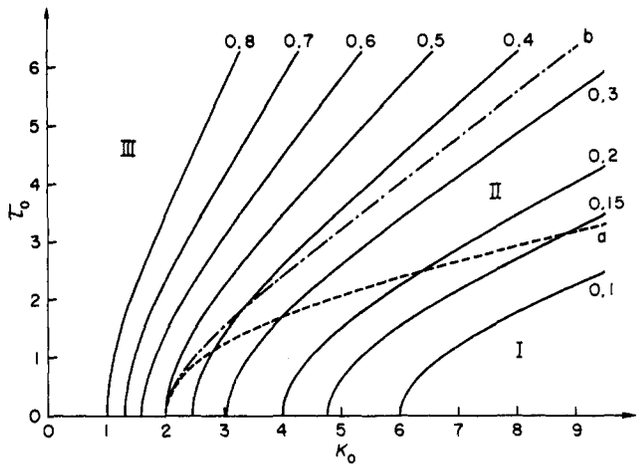

Figure 1. A family of curves with constant c_∞ in a (κ_0,τ_0) plane. The numbers attached to the curves indicate the values of c_∞. The plane is divided into three characteristic domains I, II, and III by the broken (a) and chain (b) curves (see the text).

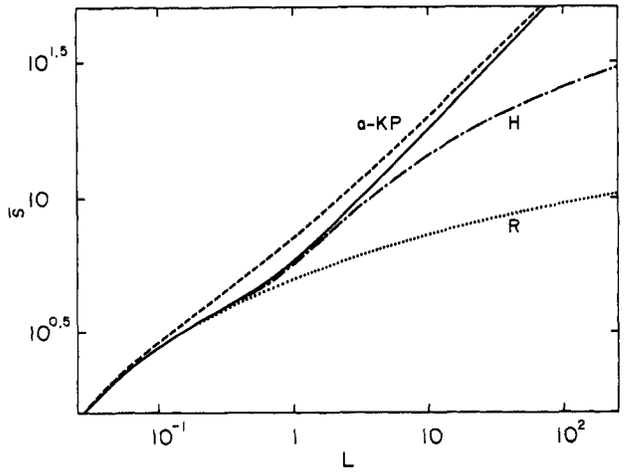

Figure 2. Double logarithmic plots of $\bar{s}$ against L. The full curve represents the values for the HW chain with $\mu = 0.2$, $\nu = 8$, and $d = 0.01$ and the broken curve a-KP, chain curve H, and dotted curve R for the associated KP chain, corresponding characteristic helix, and rod, respectively.

for the present case, in which we consider also the possible range $c_\infty^{-1}d \simeq 1$.

It is also seen that the dependences on L and d of the $\bar{s}_{\text{a-KP}}$ given by eq 25 are the same for different pairs of values of κ_0 and τ_0 when c_∞ is the same. Figure 1 shows a family of curves with constant c_∞ in a (κ_0,τ_0) plane, the numbers attached to the curves indicating the values of c_∞. The plane is divided into three domains I, II, and III, as shown in the figure, where the broken curve a is the boundary between the domains I and II and the chain curve b is the boundary between the domains II and III.[6] The ratio $\langle R^2\rangle/c_\infty t$ $(=C_n/C_\infty$ with C_n the characteristic ratio) as a function of t exhibits at least one maximum in the domains I and II, and the first peak (occurring as t is increased) is higher and lower than the coil limiting value of unity in I and II, respectively. In the domain III, the ratio is an increasing function of t but exhibits inflection in some cases. Typical HW chains belong to the domain I. Thus, Figure 1 facilitates to understand the characteristic behavior of the chain with given values of κ_0 and τ_0.

Now, it is instructive to compare the behavior of $\bar{s}$ for a typical HW chain with that for the associated KP chain; thi serves to obtain an interpolation formula for $\bar{s}$ in the next section. Figure 2 shows double logarithmic plots of $\bar{s}$ against L. The full and broken curves represent the values for the HW chain with $\mu = 0.2$, $\nu = 8$ ($\kappa_0 = 7.8384$, $\tau_0 = 1.6$, $c_\infty = 0.096471$), and $d = 0.01$, and the associated KP chain, respectively. In the figure, the values calculated from eq 53 of ref 1 for the corresponding characteristic helix and rod ($|\mu| = 1$ for the latter) are also represented by the chain (H) and dotted (R) curves, respectively. Note that the $\bar{s}$ for the regular helix and rod are functions of L/d and νd and of L/d, respectively, so that the expressions for $\bar{s}$ remain unchanged with reduced lengths. As expected from the behavior of $\langle R^2\rangle/t$ (Figures 1 and 2 of ref 3), the HW chain is seen to become the associated KP chain in the limits $L \to 0$ and $L \to \infty$, the difference being most remarkable at $L \simeq 1.0$.

Empirical Equations

From the foregoing analysis, it seems convenient to construct an interpolation formula, instead of for $\bar{s}$ itself, for a factor Γ_f defined as a function of L, d, κ_0, and τ_0 by

$$\bar{s} = \bar{s}_{\text{a-KP}}\Gamma_f(L,d;\kappa_0,\tau_0) \tag{28}$$

where $\bar{s}_{\text{a-KP}}$ is given by eq 25. A good approximation to Γ_f has been found to be of the form,

$$\Gamma_f = 1 + (A_1L^{-1/2} + A_2L^{-1})[1 - (1 + \epsilon L)e^{-\epsilon L}] + A_3Le^{-\epsilon L} \tag{29}$$

with

$$A_k = \sum_{i=0}^{3}\sum_{j=0}^{3}(\sum_{l=0}^{2}a_{ij}^{kl}d^l + a_{ij}^{k3}\ln d)\nu^j \cos(i\pi\mu) \qquad (k = 1, 2, 3) \tag{30}$$

$$a_{ij}^{12} \equiv 0 \tag{31}$$

where ϵ is a constant weakly dependent on μ and ν, and a_{ij}^{kl} are constants independent of L, d, κ_0, and τ_0. We note that the second term on the right-hand side of eq 29 has been inferred to give the analytically predicted asymptotic forms,

$$\lim_{L\to 0}\Gamma_f = 1 - (\text{constant})L \tag{32}$$

$$\lim_{L\to\infty}\Gamma_f = 1 - (\text{constant})L^{-1/2} \tag{33}$$

and the third term has been added to give good approximations for $L \lesssim 1$. Further, note that A_k are the even functions of μ. This is consistent with the fact that the transport coefficients are independent of the sense of the characteristic helix.[1]

The constants ϵ and a_{ij}^{kl} have been determined in the following way on the basis of the values of $\bar{s}$ and $\bar{s}_{\text{a-KP}}$, and therefore Γ_f, calculated from eq 14, 25, and 28 for various values of L ranging from 0.01 to 1000, and d ranging from 0.0025 to 0.25. The constants involved in eq 14 have been determined following the procedure of ref 6 for the values of κ_0 and τ_0 indicated by the filled points in the (κ_0,τ_0) plane of Figure 3. In the figure, the straight lines passing through the origin have the slopes $\mu(1 - \mu^2)^{-1/2}$, and the circles with the centers at the origin have the radii ν, the filled points as their intersections being specified by the indicated values of μ and ν. If ν is increased along one of the straight lines with a given μ, supposing that the unreduced κ_0 and τ_0 (or the actual size of the characteristic helix) are fixed, then λ decreases, and therefore the helical nature of the chain becomes strong. If μ is decreased along one of the circular arcs with a given ν (and with λ fixed), the ratio of the radius ρ to pitch h of the characteristic helix increases, and therefore again the helical nature of the chain becomes strong. This dependence on μ and ν

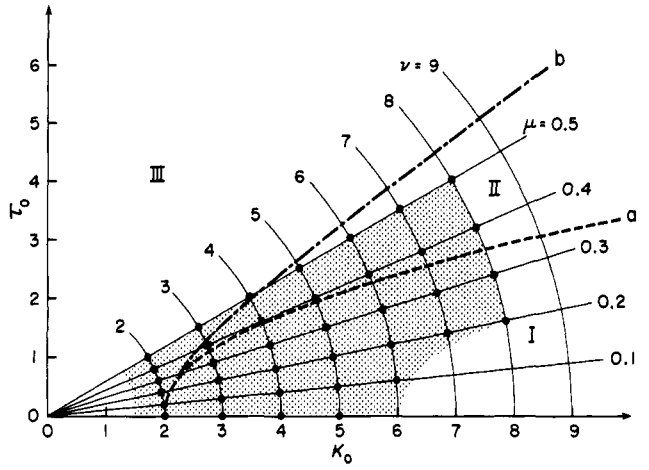

Figure 3. Straight lines passing through the origin with the slopes $\mu(1-\mu^2)^{-1/2}$ and circles with the centers at the origin and with the radii ν in the (κ_0,τ_0) plane (see also legend to Figure 1). The constants involved in eq 14 have been determined for the values of κ_0 and τ_0 indicated by the filled points. The application of eq 28 is limited to the shaded domain.

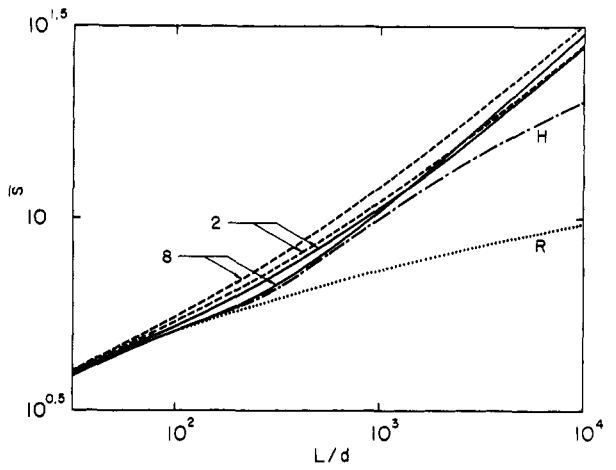

Figure 4. Double logarithmic plots of $\bar{s}$ against L/d for the two cases of $\nu = 2$ and 8 when $\mu = 0.2$ and $\nu d = 0.02$. The full and broken curves represent the values for the HW chains and the corresponding associated KP chains, respectively, the numbers attached to the curves indicating the values of ν. The chain curve H and dotted curve R represent the values for the corresponding characteristic helix and rod, respectively.

of the strength of the helical nature is useful also in a later discussion of the results. The determination of the constants in eq 14 fails for small μ and $\nu > 5$, i.e., in the domain of strong helical nature, very few real chains belonging to it.[6] The coefficients A_k (k = 1–3) in eq 29 have been determined from the values of Γ_f by the method of least squares for various sets of values of κ_0, $\tau_0(\mu,\nu)$, and d, and a best form of ϵ has been found to be

$$\epsilon = 0.3 + 0.4\nu \tag{34}$$

Then, the numerical coefficients a_{ij}^{kl} in eq 30 have been determined by the method of least squares from the values of A_k thus determined as functions of μ, ν, and d. The results for a_{ij}^{kl} are given in Table I.

The application of eq 28 with eq 29–31 and with these values of a_{ij}^{kl} is limited to the shaded domain in the (κ_0,τ_0) plane of Figure 3. This suffices for real chains; the equation for the KP chain is valid in a good approximation for $\kappa_0 \lesssim 1.5$ or for $\mu \gtrsim 0.5$ (approximately the domain III). The error in the value of $\bar{s}$ calculated from eq 28 does not exceed 1% for $L/d \geq 5$ and $0.0025 \leq d \leq 0.25$ except in the domain of strong helical nature with large d; when $L \lesssim 2$, it exceeds 1% but not 2% for $\mu = 0.2$, $\nu = 8$, and $d \geq 0.175$, for $\mu = 0.2$, $\nu = 7$, and $d \geq 0.225$, for $\mu = 0.1$, $\nu = 6$, and $d \geq 0.2$, and for $\mu = 0$, $\nu = 5$, and $d \geq 0.2$. Thus, the accuracy of eq 28 is good enough for real chains, whose d may not be regarded as large when the helical nature is strong.

Numerical Results and Discussion

In this section, we examine the change of the dependence of $\bar{s}$ on L when κ_0, $\tau_0(\mu,\nu)$, and d are changed, on the basis of the values of $\bar{s}$ calculated from eq 14 or 28. Figure 4 shows double logarithmic plots of $\bar{s}$ against L/d for the two cases of $\nu = 2$ (weak helical nature) and $\nu = 8$ (strong helical nature) when $\mu = 0.2$ and $\nu d = 0.02$. The full and broken curves represent the values for the HW chains and the corresponding associated KP chains, respectively, the numbers attached to the curves indicating the values of ν. For comparison, the values calculated from eq 53 of ref 1 for the corresponding characteristic helix and rod ($|\mu| = 1$ for the latter) are also represented by the chain (H) and dotted (R) curves, respectively. Note that the characteristic helices corresponding to the HW chains with constant μ and νd have the same $\bar{s}$ as a function of L/d. In this case, the helical nature of the chain with larger ν is stronger, as mentioned in the last section. Indeed, the curve for large ν (and small d) exhibits the helical nature remarkably; it is close to the curve for the characteristic helix in the range of small L/d and has an inflection point. This is not observed for the KP chain.

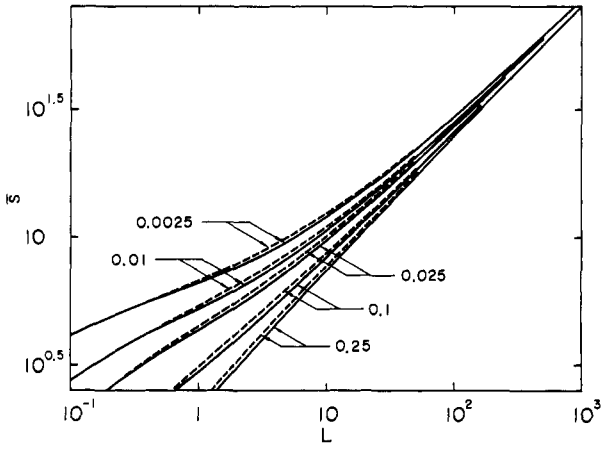

Figure 5. Double logarithmic plots of $\bar{s}$ against L for $\mu = 0.2$ and $\nu = 2$. The full and broken curves represent the values for the HW and associated KP chains, respectively, the numbers attached to the curves indicating the values of d.

In all figures in the remainder of this section, double logarithmic plots of $\bar{s}$ against L are shown for the HW and associated KP chains by the full and broken curves, respectively. Figures 5 and 6 show the dependence of the plots on d for the cases of $\mu = 0.2$ and $\nu = 2$ and of $\mu = 0.2$ and $\nu = 8$, respectively, the numbers attached to the curves indicating the values of d. From the two figures, it is seen that the difference between the HW and associated KP chains in the logarithm of $\bar{s}$ is larger for larger ν but is almost independent of d for given μ and ν. However, it is important to observe that a number of sets of values of the model parameters can give almost the same dependence of $\bar{s}$ on L. This indicates that it is impossible to determine the model parameters accurately from sedimentation coefficients s alone. In particular, the plots have the slope $^1/_2$ for $L \gtrsim 10$ in some cases, e.g., for $\nu = 2$ and $d = 0.1$ (in Figure 5) and for $\nu = 8$ and $d = 0.01$ (in Figure 6); that is, the theory predicts that for certain stiff chains, s is proportional to $M^{1/2}$ as in the case of nondraining flexible chains. In other words, even if the

Table I
Values of the Coefficients a_{ij}^{kl} in Equation 30

i	j	a_{ij}^{10}	a_{ij}^{11}	a_{ij}^{13}	a_{ij}^{20}	a_{ij}^{21}	a_{ij}^{22}	a_{ij}^{23}	a_{ij}^{30}	a_{ij}^{31}	a_{ij}^{32}	a_{ij}^{33}
0	0	2.5375 (−1)[a]	6.1968 (−1)	−1.6278 (−2)	3.3952 (−1)	−4.6385	1.4390 (1)	8.7162 (−2)	1.0508	−3.6872	1.5880 (1)	8.7802 (−3)
0	1	−3.0995 (−1)	−4.6724 (−1)	9.1389 (−3)	−1.4751 (−1)	3.6503	−1.1929 (1)	−6.9304 (−2)	−9.0414 (−1)	3.0546	−1.3388 (1)	−8.6718 (−3)
0	2	6.9453 (−2)	1.4178 (−1)	−2.5249 (−3)	3.0511 (−2)	−9.4699 (−1)	3.0947	1.6633 (−2)	1.8468 (−1)	−7.1120 (−1)	3.4091	−6.1773 (−5)
0	3	−4.2467 (−3)	−1.1603 (−2)	2.1317 (−4)	−2.8035 (−3)	7.2188 (−2)	−2.4043 (−1)	−1.2397 (−3)	−8.7902 (−3)	5.2311 (−2)	−2.3963 (−1)	3.2245 (−4)
1	0	−9.0444 (−2)	−1.5296	4.3995 (−2)	−7.9629 (−1)	9.0976	−2.6529 (1)	−1.5134 (−1)	−1.7764	5.9646	−3.9975 (1)	−1.5204 (−2)
1	1	8.1850 (−2)	1.2767	−3.6564 (−2)	6.6209 (−1)	−7.7745	2.2810 (1)	1.2396 (−1)	1.5841	−5.1252	3.3726 (1)	1.3450 (−2)
1	2	−5.5637 (−2)	−3.1646 (−1)	7.9665 (−3)	−1.3077 (−1)	1.9190	−5.7928	−3.0803 (−2)	−4.1238 (−1)	1.2759	−8.2577	−1.5675 (−3)
1	3	4.5832 (−3)	2.4625 (−2)	−5.6009 (−4)	9.1200 (−3)	−1.4272 (−1)	4.5043 (−1)	2.3187 (−3)	2.2320 (−2)	−9.0919 (−2)	5.4269 (−1)	−4.8094 (−4)
2	0	2.0821 (−1)	5.8463 (−1)	−1.6111 (−2)	2.5741 (−1)	−4.5052	1.3826 (1)	7.8755 (−2)	9.2178 (−1)	−4.1242	1.7729 (1)	1.4576 (−2)
2	1	−1.7080 (−1)	−4.9407 (−1)	1.3292 (−2)	−2.0122 (−1)	3.8257	−1.1855 (1)	−6.4171 (−2)	−7.6699 (−1)	3.4797	−1.5089 (1)	−1.1597 (−2)
2	2	3.9225 (−2)	1.3372 (−1)	−3.3450 (−3)	4.8619 (−2)	−9.6943 (−1)	3.0397	1.5661 (−2)	1.7242 (−1)	−8.4744 (−1)	3.8234	1.2472 (−3)
2	3	−2.5803 (−3)	−1.0999 (−2)	2.5427 (−4)	−3.9752 (−3)	7.2863 (−2)	−2.3556 (−1)	−1.1814 (−3)	−8.9529 (−3)	6.0990 (−2)	−2.7183 (−1)	2.6641 (−4)
3	0	−1.0637 (−1)	−1.8923 (−1)	6.6103 (−3)	−1.2949 (−1)	1.9356	−5.7137	−3.5178 (−2)	−5.8322 (−1)	2.3079	−7.4646	−1.7493 (−2)
3	1	1.0068 (−1)	1.4892 (−1)	−5.0745 (−3)	9.1012 (−2)	−1.6424	4.9238	2.8830 (−2)	5.0578 (−1)	−1.9798	6.1117	1.5518 (−2)
3	2	−2.8348 (−2)	−3.7321 (−2)	1.1276 (−3)	−1.6774 (−2)	4.1452 (−1)	−1.2730	−7.0222 (−3)	−1.2119 (−1)	4.9551 (−1)	−1.4238	−3.4461 (−3)
3	3	1.9100 (−3)	3.0521 (−3)	−8.3416 (−5)	1.3340 (−3)	−3.1409 (−2)	1.0111 (−1)	5.2759 (−4)	6.3503 (−3)	−3.6803 (−2)	8.1336 (−2)	8.7347 (−5)

[a] $a(n)$ means $a \times 10^n$.

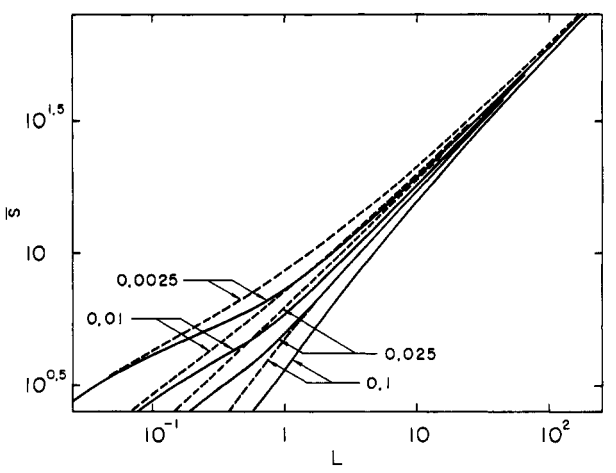

Figure 6. Double logarithmic plots of $\bar{s}$ against L for $\mu = 0.2$ and $\nu = 8$; see legend to Figure 5.

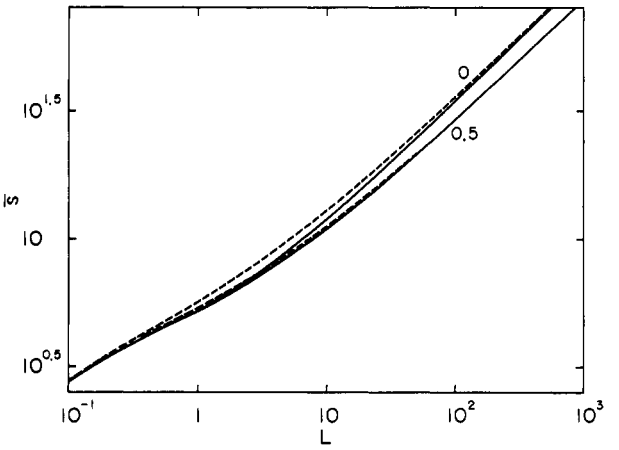

Figure 7. Double logarithmic plots of $\bar{s}$ against L for $\nu = 3$ and $d = 0.01$. The full and broken curves represent the values for the HW and associated KP chains, respectively, the numbers attached to the curves indicating the values of μ.

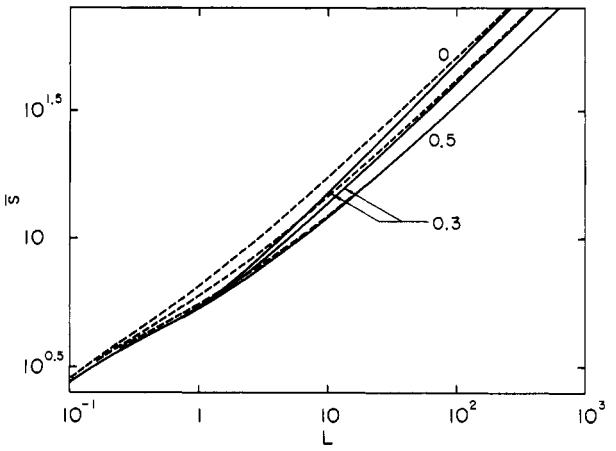

Figure 8. Double logarithmic plots of $\bar{s}$ against L for $\nu = 5$ and $d = 0.01$; see legend to Figure 7.

proportionality of s to $M^{1/2}$ is observed experimentally, the chain may not always be regarded as a random coil but may possibly be characterized as an HW chain. A definite conclusion regarding the characterization of a given chain or the accurate determination of its model parameters requires also an analysis of other transport coefficients.

Figures 7–9 show the dependence of the plots on μ for $\nu = 3$, 5, and 7, respectively, with d being fixed at 0.01, the numbers attached to the curves indicating the values of μ. In this case (for which d is fixed), all the plots yield the

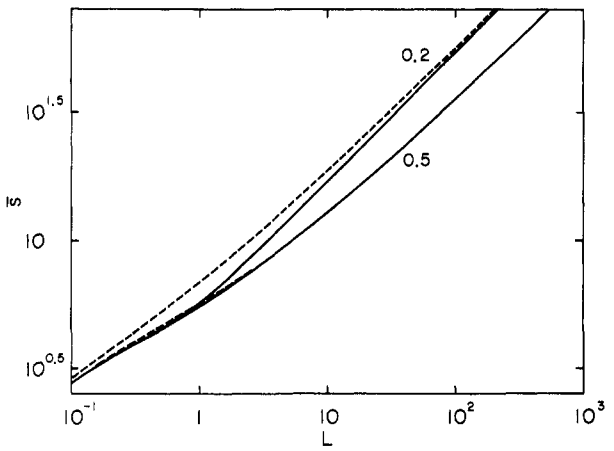

Figure 9. Double logarithmic plots of $\bar{s}$ against L for $\nu = 7$ and $d = 0.01$; see legend to Figure 7.

same $\bar{s}$ corresponding to the rod in the limit $L \to 0$. It is seen that this dependence is larger for larger ν, and also that the difference between the HW and associated KP chains in $\bar{s}$ is larger for smaller μ (for stronger helical nature) irrespective of the values of ν and is negligibly small for $\mu \gtrsim 0.5$ provided that $L \gtrsim 10$. This implies that the equation for the KP chain is valid in a good approximation for $\mu \gtrsim 0.5$ irrespective of the values of d, as mentioned already.

Finally, it is possible to make also the plots which show the dependence on ν for various values of μ with d fixed. If ν is increased at constant μ, supposing that λ is fixed, then the unreduced κ_0 and τ_0 increase at constant κ_0/τ_0, and therefore the unreduced ρ and h decrease at constant ρ/h (with the unreduced d fixed). However, such a variation of the parameters leads to no salient and systematic change of the plots, and therefore we do not show them.

Conclusion

We have presented the useful empirical formula for the translational friction and diffusion (or sedimentation) coefficients of helical wormlike cylinders on the basis of the theoretical values evaluated by the Oseen–Burgers procedure with the preaveraged Oseen tensor. The analysis of the results shows that it is difficult to determine the model parameters accurately from, for instance, sedimentation coefficients alone, and especially that certain stiff (helical wormlike) chains may exhibit the same dependence of the sedimentation coefficient of the molecular weight as flexible chains. Thus, a study of the intrinsic viscosity and also other transport coefficients of helical wormlike chains is required. It is then suggested that there is a possibility of interpreting consistently some experimental data for both the intrinsic viscosity and sedimentation coefficient on the basis of the helical wormlike chain even when the assumption of the random coil or of the wormlike model fails.

References and Notes

(1) H. Yamakawa, T. Yoshizaki, and M. Fujii, *Macromolecules*, **10**, 934 (1977).
(2) H. Yamakawa and M. Fujii, *J. Chem. Phys.*, **64**, 5222 (1976).
(3) H. Yamakawa, *Macromolecules*, **10**, 692 (1977).
(4) H. Yamakawa and M. Fujii, *Macromolecules*, **6**, 407 (1973).
(5) J. G. Kirkwood and J. Riseman, *J. Chem. Phys.*, **16**, 565 (1948).
(6) H. Yamakawa, J. Shimada, and M. Fujii, *J. Chem. Phys.*, **68**, 2140 (1978).
(7) H. Yamakawa, M. Fujii, and J. Shimada, *J. Chem. Phys.*, **65**, 2371 (1976).
(8) H. Yamakawa and J. Shimada, *J. Chem. Phys.*, **68**, 4722 (1978).

Molecular Weight and Carbon-14 Distributions of Poly(2-alkylbutadienes) Obtained in the Presence of Bis[(π-crotyl-^{14}C)nickel iodide]

L. A. Churlyaeva, V. I. Valuev, V. S. Bodrova, T. S. Dmitrieva, M. I. Lobach, and V. A. Kormer*

S. V. Lebedev Synthetic Rubber Research Institute, Leningrad, 198035, USSR.
Received July 27, 1978

ABSTRACT: The MWD and ^{14}C distribution of poly(2-alkylbutadienes) obtained in the presence of bis[(π-crotyl-^{14}C)nickel iodide] in benzene solution has been studied. It is shown that both the polymer chain length and the nature of the 2-alkyl substituent in polydiene play a decisive role in determining the dissociation degree of dimeric π-allylic active sites. The correlation between MWD and the ratio of the monomeric species of active sites to the dimeric ones is established.

In our previous study[1] we suggested that the mode of MWD of polybutadienes formed in the presence of bis(π-crotylnickel iodide) is determined not only by the "living" chain mechanism operative in this reaction but also by the recombination effects observed during the deactivation of active sites. The recombination itself is dictated, first, by the π-allylic nature of active sites and, second, by their dimeric state. The growth of the molecular weight of "living" macromolecules should favor ever increasing dimer–monomer dissociation.

The importance of the investigations of diolefine transformations catalyzed by allylic systems to the understanding of the ionic coordination catalysis encouraged us to study the polymerization of 2-alkylbutadiene homologues whose behavior in these reactions was found to have some important distinguishing features.[2]

Experimental Section

The experimental procedure used was previously described.[1] 2-Ethyl- and 2-isopropylbutadienes were prepared by pyrolysis of the corresponding 2-alkyl-3-acetoxy-1-butenes.[3] Polymerization of isoprene was carried out in a 3.0-L stainless steel autoclave at 40 °C. Polymerization of 2-ethyl- and 2-isopropylbutadienes was conducted in glass ampules at 20 °C. The number-average molecular weights of polymers and also of adducts of π-crotylnickel

0024-9297/79/2212-0038$01.00/0